ACS APPLIED POLYMER MATERIALS

pubs.acs.org/acsapm

Article

Microporous Polymeric Networks Containing a Long-Term Stable Au^I Catalyst for Enyne Cyclization

Sandra Rico-Martínez, Adrián Ruiz, Beatriz López-Iglesias, Cristina Álvarez, Ángel E. Lozano, and Jesús A. Miguel*

Cite This: *ACS Appl. Polym. Mater.* 2024, 6, 2453−2463

Read Online

ACCESS | Metrics & More | Article Recommendations | Supporting Information

ABSTRACT: Two microporous polymer networks having a confined Au^I carbene catalyst were obtained and tested for the skeletal rearrangement of enynes. These catalysts were obtained from precursor porous organic polymers (POPs), a type of microporous polymer network, synthesized by the reaction of isatin or a mixture of isatin/trifluoroacetophenone (1:1) with triptycene (**POP1** and **POP2**, respectively) through an electrophilic aromatic substitution, EAS, reaction promoted by trifluoromethanesulfonic acid. These precursors could be easily functionalized through the lactam moiety to form Au^I carbene catalysts (**POP1-AuCarbene** and **POP2-AuCarbene**). The confined carbenes proved to be very active for the skeletal rearrangement of dimethyl 2-(3-methyl-2-butenyl)-2-propinylmalonate enyne. A large increase in the stability of the Au^I catalysts was observed compared to those of most of the homogeneous catalysts described so far in the bibliography. This long-term stability was associated with the separation of Au^I atoms, induced by their confinement in the microporous networks. In particular, **POP2-AuCarbene** exhibited outstanding long-term stability, maintaining catalytic activity even after several months.

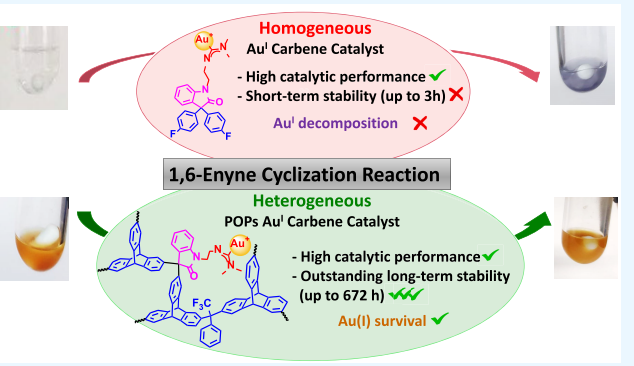

KEYWORDS: *porous organic polymers, Au^I catalyst, Au^I stability, confined catalyst, enyne cyclization*

1. INTRODUCTION

The design of catalysts for organic synthesis that are more efficient, have a low environmental impact, and, at the same time, are very stable over time and in a large number of processes is highly demanded by chemical industries. In addition, in the case of organometallic catalysts, it is also necessary, especially when the synthesis is aimed at obtaining a pharmaceutical compound in which leaching of the metal is as low as possible for both medical and economic reasons. One of the most interesting approaches, particularly when the goal is to reduce certain drawbacks, is to design and obtain materials of heterogeneous nature, i.e., using a catalyst supported or embedded in an insoluble material in the reaction medium, which will improve the recovery after the reactive process.

A wide variety of materials have been employed as heterogeneous catalysts, such as zeolites,[1] polymeric resins,[2,3] oxides,[4−6] silicas,[7−9] metal−organic frameworks (MOFs),[10,11] covalent−organic frameworks (COFs),[12,13] or porous organic polymers (POPs).[14−20] Contrary to MOFs and COFs, which are crystalline, POPs are amorphous materials, which results in a wider distribution of the pore size. In this context, POPs have gained attention in many applications such as gas storage,[21] separation,[22] and catalysis[23] due to their high specific surface areas, tunable pore size, and easy functionalization.[16,23] Recently, our group has developed a low-cost methodology for preparing POPs by polycondensation reactions made by electrophilic aromatic substitution (EAS) between a ketone presenting electron-withdrawing groups and trifunctional rigid aromatic monomers. The resulting POPs presented high microporosity, with Brunauer−Emmett−Teller (BET) surface areas of up to 800 $m^2\ g^{-1}$, and outstanding thermal stability (superior to 450 °C).[24] These POPs have also proven to be good supports for heterogeneous catalysts.[25,26]

Looking at a specific field of catalysis, in the last 2 decades, Au^I complexes have emerged as exceptional catalytic materials[27−31] for the activation of alkynes[32,33] and, in particular, enynes,[34−40] which has permitted the obtainment of a wide variety of cyclic products used in synthetic chemistry as starting compounds.[41] Au^I complexes, of the [AuXL] type, are usually used for these reactions, which in the presence of a Ag salt, acting as a halide extractor, leads to the formation of a *naked gold* $[AuL]^+$ that acts as a very soft and active electrophile. This synthetic methodology requires an auxiliary

Received: September 12, 2023
Revised: January 24, 2024
Accepted: January 25, 2024
Published: February 15, 2024

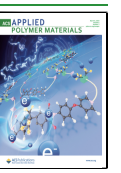

https://doi.org/10.1021/acsapm.3c02174
ACS Appl. Polym. Mater. 2024, 6, 2453−2463

ligand L able to stabilize the Au^I system under the conditions in which the catalysis takes place. For this reason, the [AuXL] complexes used in catalysis require a strong ligand [phosphines, N-heterocyclic carbenes (NHCs),[42,43] etc.] that stabilizes the metal center. As an alternative to conventional Au^I NHCs, hydrogen-bond-supported heterocyclic carbenes (HBHCs)[44] are suitable ligands because they are easily achieved by a mere nucleophilic addition of primary amines to isocyanides, which shows a great advantage over the complicated preparation of NHCs obtained by transmetalation from Ag. In a comparative study,[45] it was observed that N-acyclic carbenes (NACs)[46] were also valid for the skeletal rearrangement of 1,6-enynes, similar to HBHCs, showing the advantage of an easy modulation of their steric and electronic characteristics, which has given rise to an intense search of Au^I catalysts that can be obtained by employing these preparation methods.[47,48] Chart 1 shows the types of Au^I carbene complexes.

Chart 1. Types of Au^I Carbene Complexes

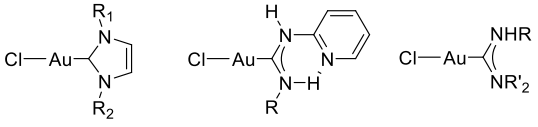

It is well-known that, in the majority of catalysts with Au^I-based systems, decomposition to Au^0 (after extraction of the halide in the absence of reducing agents) is observed, and therefore the loss of catalytic activity. The reduction occurs due to the disproportionation of three Au^I atoms to give two Au^0 and one Au^{III} atoms, a reaction that was known[49] and has been used in the synthesis of some Au^{III} carbenes.[50−55]

Despite the fact that the homogeneous-catalyzed cyclization of 1,6-enynes has been extensively studied, this reaction has been marginally studied in heterogeneous conditions. However, it has been proven that when the catalyst is immobilized into a polymer, the product selectivity differs significantly compared to that of a homogeneous catalyst.[56] These results, added to the easy recovery of the catalyst, are a promising solution to green and sustainable development in the chemical industry.[5,6,17,30,57]

In this work, we report the formation of a catalytic Au^I material where a NAC has been confined into microporous polymer networks. POPs have shown great efficiency as heterogeneous catalysts, thanks to properties such as their high microporosity, and when a polymer material has been chosen, they show excellent thermal and chemical stability.[58] Essentially, the simplified approach employed in this work consisted of making a heterogeneous catalytic Au^I NAC by anchoring it onto a lactam group present in micro-POPs by using an ethylenic spacer between both moieties. The catalytic properties of these Au^I materials were evaluated for the cyclization of 1,6-enynes. Confining the catalyst into a network polymer would allow its use in greener and environmentally friendly processes.[59] More importantly, the carbene molecules anchored inside the polymeric network will be sufficiently separated, which would prevent an approach between the Au^I atoms, leading to a decrease of Au^I degradation and consequently to a great improvement of the catalyst stability over time.[14] This fact is crucial because, although these organometallic catalysts are exceptionally good for a wide variety of catalytic processes, the existence of disproportionation processes between Au^I atoms severely limits their use in industry.[55]

2. EXPERIMENTAL PART

2.1. Materials. All reactions were performed under dry N_2. The reactions using Ag salts were carried out shielded from light. *N*-(2-Bromoethyl)-2-phthalimide was prepared as described in the literature.[60,61] Chloro(tetrahydrothiophene)gold(I) ([AuCl(THT)]) was synthesized according to the reported methodology.[62] The rest of the reactants are commercially available. Isatin (1*H*-indol-2,3-dione, 98%) and trifluoroacetophenone (TFAP, 97%) were purchased from Alfa Aesar. Fluorobenzene (FBenz, 99%) and trifluoromethanesulfonic acid (TFSA, 99%) were purchased from FluoroChem. Triptycene (TRP, 97%) was purchased from ABCR. Formic acid (98%) was purchased from PanReac. Triethylamine (NEt_3, 99%) and triphosgene (99%) were purchased from Acros. Dimethylamine (solution 2 M in tetrahydrofuran) and tosyl chloride (99%) were purchased from Alfa Aesar. *N*-Methylpyrrolidine anhydrous (99%), chloroform anhydrous ($CHCl_3$, 99%), and toluene anhydrous (99%) were purchased from Sigma-Aldrich. Hydrazine hydrate (analytical reagent grade) was purchased from Fisher Scientific.

2.2. Techniques. The NMR spectra were recorded with Bruker Avance 400 Ultrashield, Varian 400-MR, and Varian 500/54 Premium Shielded instruments at 25 °C by using $CDCl_3$ and CD_2Cl_2 as solvents. The elemental C, H, and N analyses were carried out on an Elemental Carlo Erba 1108/combustion chromatograph. Fourier transform infrared (FT-IR) spectroscopy was performed with a PerkinElmer Frontier spectrometer coupled to a Pike GladiATR-210 accessory. Solid-state (SS) ^{13}C cross-polarization magic-angle-spinning NMR (CP/MAS ^{13}C NMR) spectra were recorded on a Bruker Advance 400 spectrometer equipped with an 89 mm wide bore and a 9.4 T superconducting magnet. The spectrometer was operated at a Larmor frequency of 100 MHz by using a contact time of 1 ms and a delay time of 3 s. All samples were spun at 11 kHz. Thermogravimetric analysis (TGA) was performed on a TA Q-500 thermobalance under a N_2 atmosphere (60 mL min^{-1}). Dynamic TGA was carried out using the Hi-Res method (sensitivity and resolution parameters 1 and 4, respectively), ramping at 20 °C min^{-1} from 30 to 850 °C. Scanning electron microscopy (SEM) images were taken with a Quanta 200 FEG ESEM microscope (FEI, Hillsboro, OR) on Au-metallized samples operating at an acceleration voltage of 1.5 kV under high vacuum and using the detection of secondary electrons method. Transmission electron microscopy (TEM) images were acquired with a JEM 1011HR apparatus operating at an acceleration voltage of 100 kV. The Au content was determined by inductively coupled plasma optical emission spectroscopy (ICP-OES), carried out with a Varian 725-ES Radial Simultaneous Radial ICP-OES atomic emission spectrophotometer. Additionally, the Au content was also determined by dynamic TGA under an air atmosphere, taking the residue at 850 °C, ramping at 20 °C min^{-1} from 300 to 850 °C. Porous texture characterization of the polymers was carried out from their N_2 adsorption−desorption isotherms measured at −196 °C in a ASAP 2010 volumetric device (Micromeritics) in the 10^{-6}−0.995 relative pressure (P/P_0) range. The minimum equilibrium time (for both adsorption and desorption) was 300 s. Samples were degassed at 125 °C for 18 h, under vacuum, before sorption measurements, to obtain the apparent surface area (S_{BET}) by applying the BET method in the 0.01−0.2 P/P_0 range, the micropore volume (V_{micro}) using the Dubinin−Radushkevich equation in the 0.005−0.1 range, and the total pore volume (V_{total}) as the volume of liquid nitrogen adsorbed at 0.975 relative pressure. X-ray diffraction (XRD) was determined by an Agilent Supernova diffractometer with an Atlas CCD area detector. Data collection was performed with Mo Kα radiation (λ = 0.71073 Å) or Cu Kα radiation (λ = 1.54184 Å). Data integration, scaling, and empirical absorption correction were carried out using the *CrysAlisPro* program package.[63] The structures were solved using direct methods and refined by full-matrix least squares against F^2 with *SHELX* in *OLEX2*.[64] The non-H

https://doi.org/10.1021/acsapm.3c02174
ACS Appl. Polym. Mater. 2024, 6, 2453−2463

Scheme 1. Synthesis of Precursor Polymers POP1 (A) and POP2, (B), Model M1 (C), and Heterogeneous (A and B) and Homogeneous (C) Au Catalysts[a]

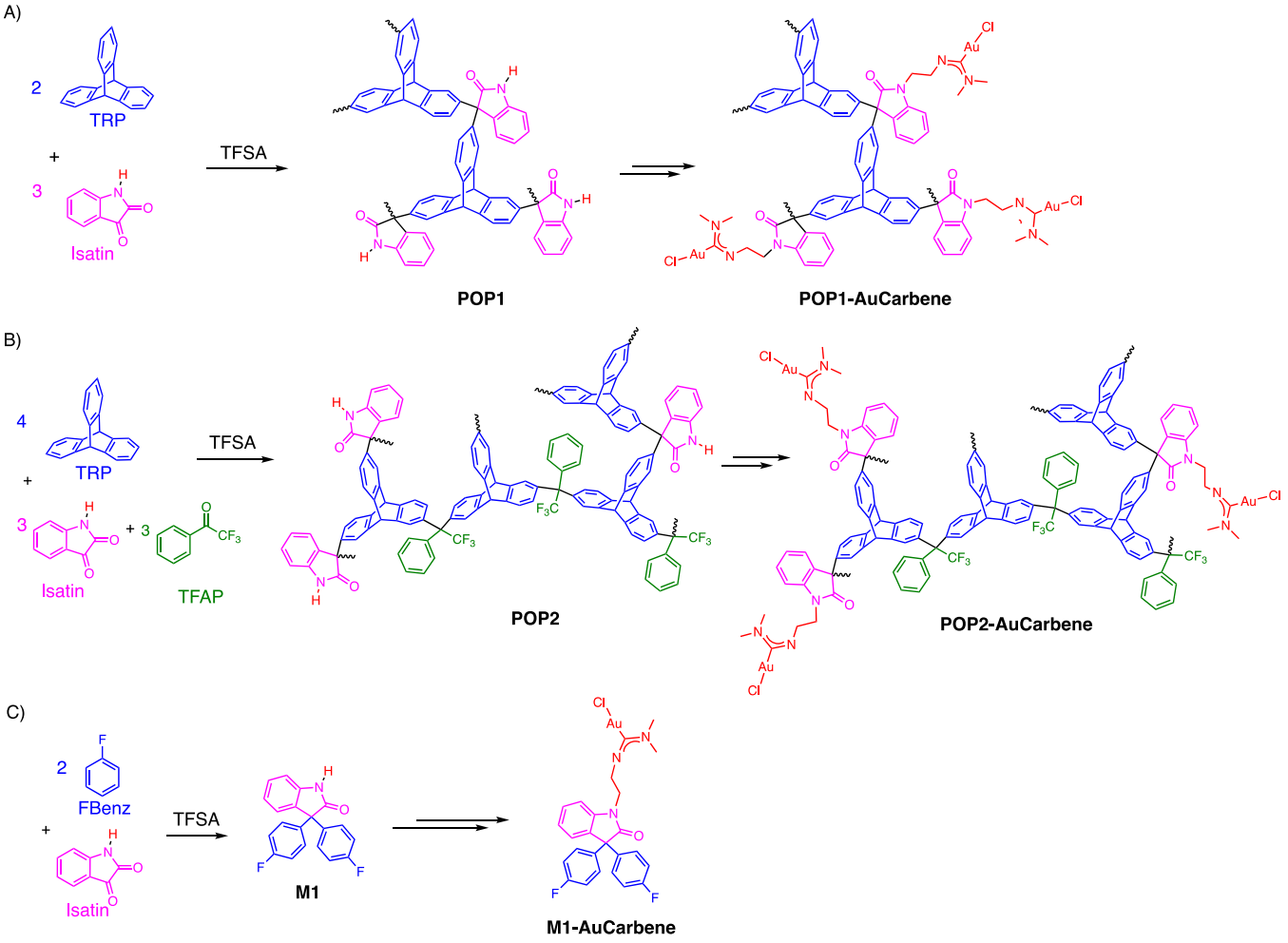

[a]The numbers next to the monomer structures indicate the number of moles employed in the reaction.

Scheme 2. Conversion of Precursors to AuCarbene Catalysts

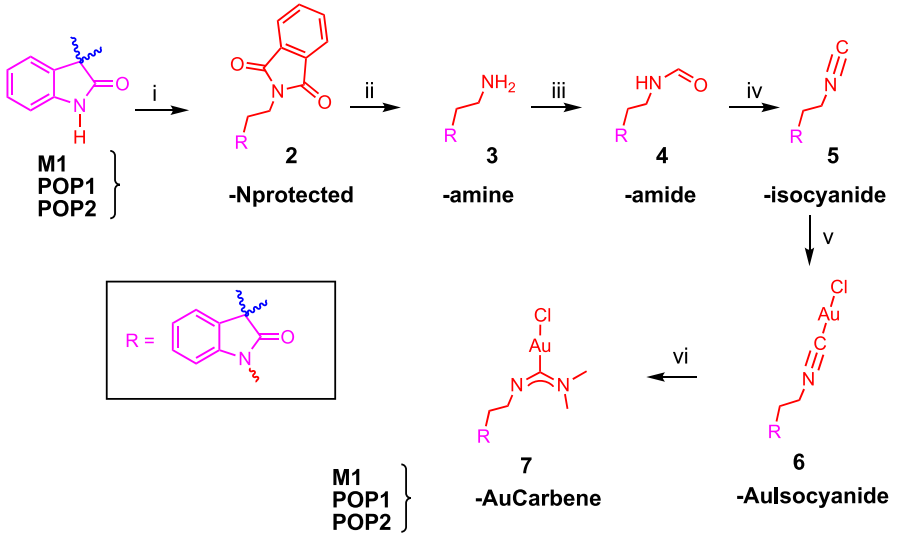

atoms were refined anisotropically, and the H atoms were placed at idealized positions and refined using the riding model. Refinement proceeded smoothly to give the residuals shown in Tables S3−S8 (section S4). Crystallographic data for the structures reported in this paper have been deposited with the Cambridge Crystallographic Data Centre as Supplementary publications with the deposition numbers

https://doi.org/10.1021/acsapm.3c02174
ACS Appl. Polym. Mater. 2024, 6, 2453−2463

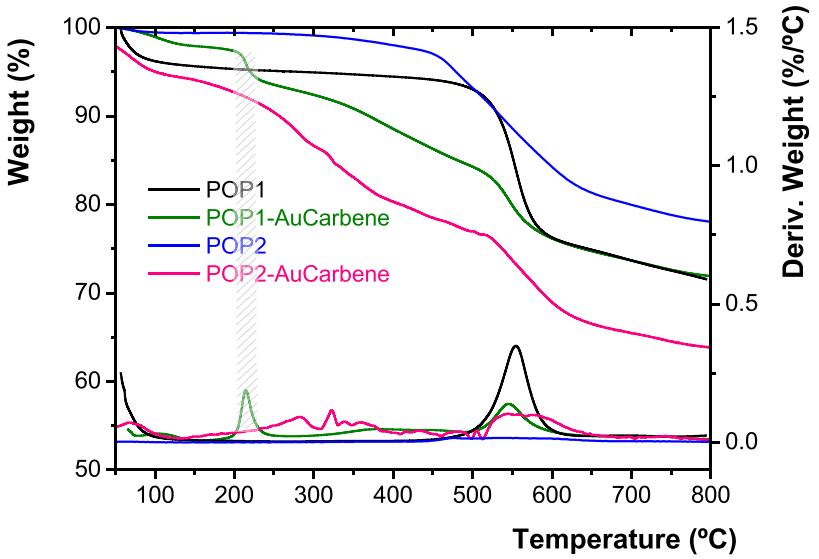

Figure 1. TGA curves in a N_2 atmosphere of the precursor polymers and heterogeneous catalysts.

CCDC 2267959 (**M1**), 2267960 (**M2**), 2267961 (**M5**), 2267962 (**M6**), and 2267963 (**M7**).

3. RESULTS AND DISCUSSION

3.1. Synthesis of Heterogeneous Confined Catalysis. The precursor microporous polymer networks (**POP1** and **POP2**) were synthesized by a polycondensation reaction (EAS-based reaction) between TRP and the isatin ketone (for **POP1**) or an equimolar mixture of isatin/TFAP ketones (in the case of **POP2**) in a stochiometric ratio, accordingly with each functionalization (TRP:ketone ratio = 2:3), employing TFSA as a promoter, as represented in parts A and B of Scheme 1, respectively. The idea of making the copolymer **POP2** is to reduce the number of isatin groups (a 50% molar ratio) in the macromolecular structure and, consequently, to decrease the theoretical amount of Au^I in the catalytic material, obtaining a cheaper material and, more importantly, increasing the distance between Au atoms, getting catalysts with long-term stability. Additionally, to optimize the formation reaction of the Au^I catalyst into the polymer network and also to assess the catalytic activity and stability of the structural unit, a homogeneous model catalyst (**M1**) resembling the structure of the precursor POP was prepared. **M1** was synthesized by the condensation reaction of isatin with 2 equiv of FBenz in the presence of TFSA, as shown in Scheme 1C.

Due to the presence of the lactam moiety of isatin, formed during the EAS reaction, which has a relatively acidic H atom, POPs could be easily functionalized,[65,66] in a short number of steps, to produce Au^I carbene-confined catalysts. The chemical structures of the final precatalytic materials (before extraction of the halide) **POP1-AuCarbene**, **POP2-AuCarbene**, and **M1-AuCarbene** are shown in Scheme 1 (parts A−C, respectively). Functionalization of the precursor polymers into AuCarbene materials was carried out by a straightforward and regioselective multistep process, whose synthetic route is represented in Scheme 2.

In the first stage (stage i), the lactam N−H group of the precursor derivative, **M1**, **POP1**, or **POP2**, gave the protected amine lactam-modified derivative **2** (phthalamide derivative) by nucleophilic substitution, which presents the ethylenic spacer. Then, hydrazine was employed to deprotect the phthalamide group, giving rise to the amine **3** (stage ii), which was transformed into a formamide derivative **4**, employing formic acid (stage iii). Subsequently, isocyanide **5** was formed from **4** by dehydration with triphosgene in the presence of NEt_3 (in the case of the model) or tosyl chloride in a pyridine medium (for polymer networks) (stage iv). By the reaction of **5** with [AuCl(THT)] in a 1:1 ratio, AuIsocyanide **6** was obtained (stage v). Finally, catalytic Au^I carbene **7** was prepared by the nucleophilic attack of **6** with dimethylamine (stage vi). Details of the synthesis of the model and polymer networks and their functionalization into the catalyst are thoroughly described in section S1. The XRD structures of **M1**, **M2** (**M1-Nprotected**), **M5** (**M1-Isocyanide**), **M6** (**M1-AuIsocyanide**), and **M7** (**M1-AuCarbene**) confirmed the proposed structures in Scheme 2 and are represented in section S2. Functionalization of the model into a AuCarbene was quantitative, whereas those for the polymer and copolymer were 63% and 46%, respectively, according to the Au content determined by ICP-OES.

3.2. Characterization of the Au^I Carbene POP Catalysts (POP-AuCarbene). The precursor polymers, **POP1** and **POP2**, were obtained in practically quantitative yields. The thermal stability of both polymer precursors was very high, with the onset of the degradation temperature above 500 °C under a N_2 atmosphere, with carbonaceous residue above 70% at 800 °C under a N_2 flow. The POPs-AuCarbene catalysts showed lower thermal stability, around 200 °C, due to the degradation of the catalyst carbene moiety, while the char yield under a N_2 atmosphere remained high compared to those of the precursors. As an example, Figure 1 shows the TGA curves in a N_2 atmosphere of the POP precursors and the final catalysts (POPs-AuCarbene). This figure shows, for both catalytic materials, a weight loss between 200 and 425 °C, which can be associated with degradation of the unit incorporating the carbene. After this degradation, the materials presented a behavior analogous to that observed in the nonfunctionalized precursor polymeric networks. The TGA results of all of the intermediate materials are shown in Figures S27 and S28.

FT-IR and SS ^{13}C NMR analyses confirmed the functionalization of the precursors POPs. The FT-IR technique was

https://doi.org/10.1021/acsapm.3c02174
ACS Appl. Polym. Mater. 2024, 6, 2453−2463

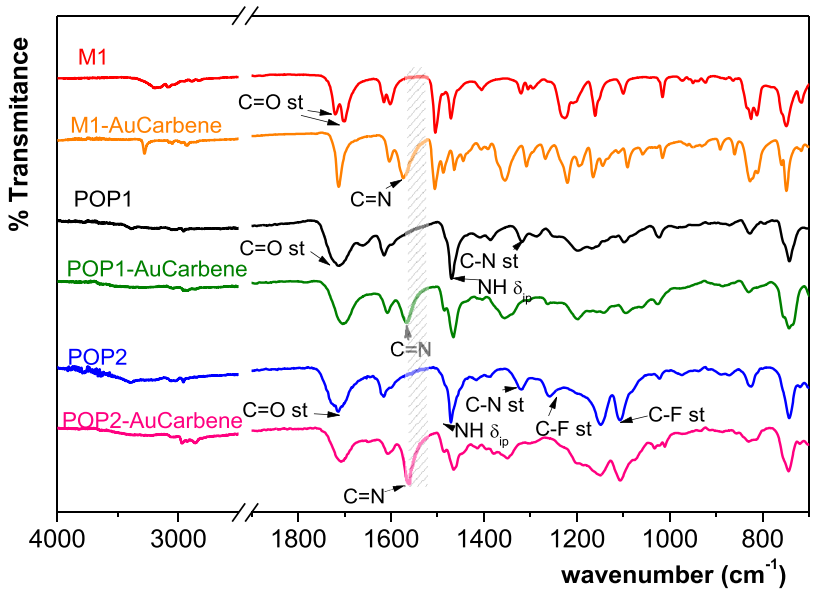

Figure 2. FT-IR spectra of the POP precursors and final catalytic materials.

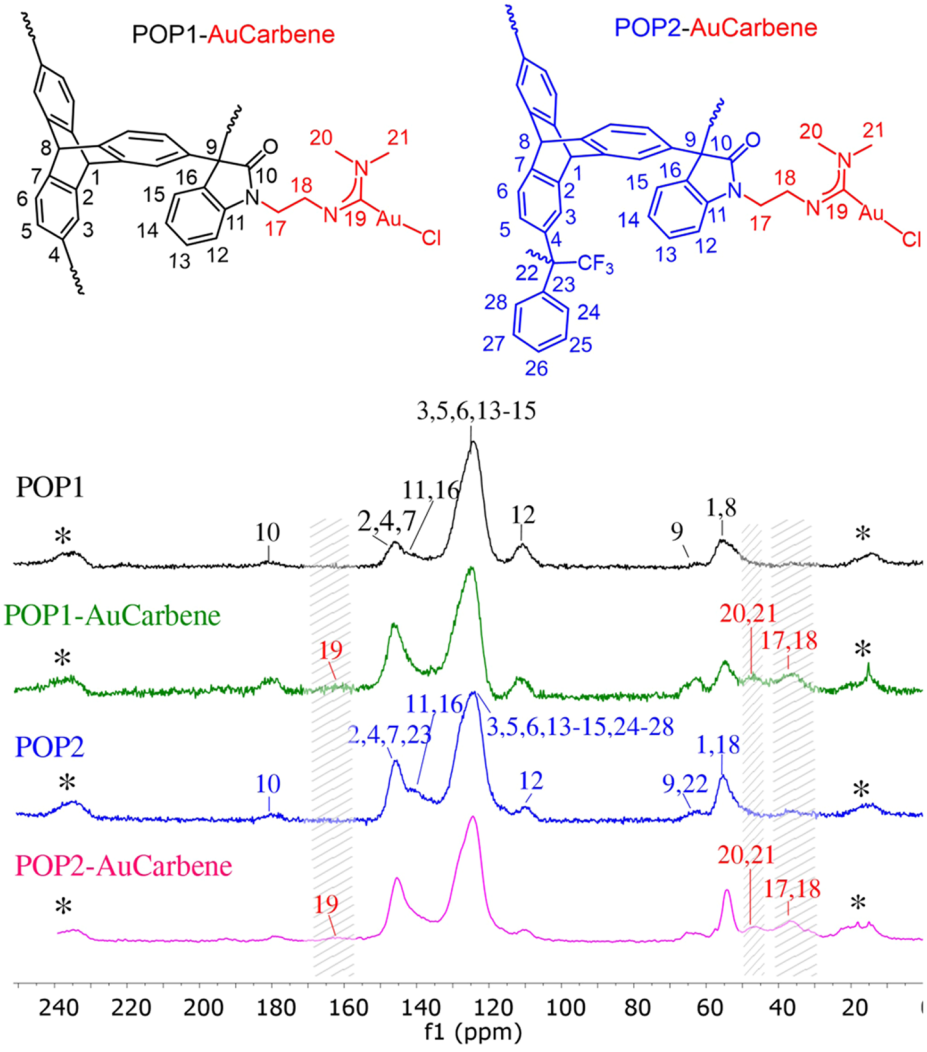

Figure 3. CP/MAS ^{13}C NMR spectra of precursor POPs and AuCarbene materials. *Spinning side bands.

critical for the synthesis procedure because the appearance or disappearance of certain typical bands of functional groups allowed us to know when the reaction had finished. As can be seen in Figure S1 (for **M1** modification), Figure S29 (for

https://doi.org/10.1021/acsapm.3c02174
ACS Appl. Polym. Mater. 2024, 6, 2453−2463

POP1 modification), or Figure S30 (for **POP2** modification), each intermediate compound presents at least one relevant signal in FT-IR. So, compound **2** (N-protected) presents the typical band of C═O coming from the phthalimide at ca. 1770 cm^{-1}. Compound **3** (amine), the product of deprotection, can be followed by the disappearance of the phthalimide C═O band. The amide compound **4** shows a band coming from the carbonyl of formamide, at 1660 cm^{-1}. The N≡C band of the isocyanide derivative **5** appeared at ca. 2150 cm^{-1}, and it is moved to ca. 2250 cm^{-1} due to Au^{I} coordination in AuIsocyanide **6**. Finally, AuCarbene **7** presents the disappearance of the isocyanide band and the appearance of a C═N vibration at ca. 1566 cm^{-1}. As an example, Figure 2 represents the FT-IR spectra of precursors **M1**, **POP1**, and **POP2** and the final catalytic materials **M1-AuCarbene**, **POP1-AuCarbene**, and **POP2-AuCarbene**, in which the appearance of a band at 1566 cm^{-1} can be observed as corresponding to the C═N bonds.

SS ^{13}C NMR characterization was also useful for verifying the chemical modification. Figures S31 and S32 show SS ^{13}C NMR spectra from POPs to POPs-AuCarbene. As an example, the CP/MAS ^{13}C NMR spectra of precursors POPs and the final POPs-AuCarbene catalysts are represented in Figure 3, in which two additional bands compared to pristine POPs at 165 ppm (C19, low intensity) and 48 ppm (C20 and C21) can be observed, due to the C═N bonds and methyl groups, respectively, coming from the carbene moiety. The additional peak at 36 ppm (C17 and C18) is due to the methylene linkers that connect the isatin with the carbene moiety.

The surface morphologies of microporous polymer networks (precursors and AuCarbenes) were examined by field-emission

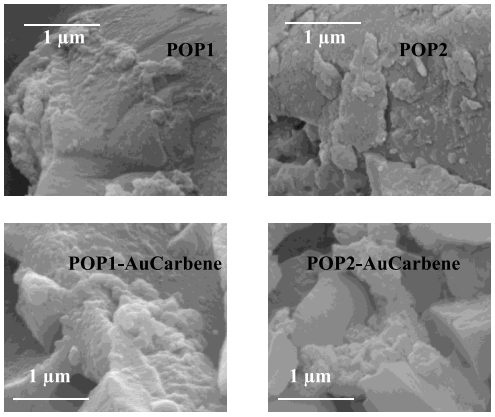

Figure 4. FE-SEM images of the precursors POPs and precatalyst POPs-AuCarbenes.

SEM (FE-SEM) and are represented in Figure 4. TEM images determined that the POP networks consisted of clusters of small nanoparticles (less than 200 nm; Figure S33).

The porosity of the precursor POPs was determined by low-pressure adsorption measurements using N_2 adsorption at −196 °C. **POP1** and **POP2** showed specific BET surface areas of 926 and 263 $m^2\ g^{-1}$, respectively. N_2 adsorption−desorption isotherms measured at −196 °C for POPs and POPs-AuIsocyanide are represented in Figures S34 and 5, respectively. These polymer networks showed a microporous character and a significant hysteresis, which was more remarkable for **POP2** and the **POP2-AuIsocyanide** catalyst. These types of isotherms have been reported for other

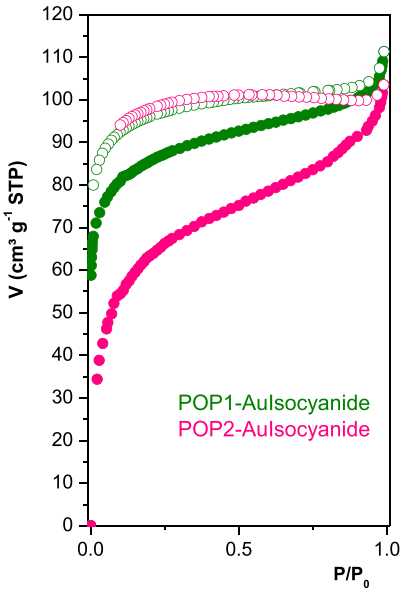

Figure 5. N_2 adsorption (full symbols)−desorption (empty symbols) isotherms measured at −196 °C for POPs-AuIsocyanide.

microporous networks.[24] The Au^{I} isocyanide POPs showed lower specific surface areas than those of the precursors, but the BET values were high enough (323 $m^2\ g^{-1}$ for **POP1-AuIsocyanide** and 246 $m^2\ g^{-1}$ for **POP2-AuIsocyanide**), with average pore diameters of 2.0 and 2.5 nm, respectively. The pore-size distributions of both precursors POPs and POPs-AuIsocyanide are shown in Figure S36. The resulting AuIsocyanides anchored in the POP showed high microporosity, being higher for **POP2-AuIsocyanide** than for **POP1-AuIsocyanide** (93% and 50% respectively), as shown in Table 1.

It should be noted that it was not possible to perform adsorption−desorption isotherms for the Au-NHC POP carbenes because a large disparity of values was observed, probably due to decomposition during the overnight conditioning (degassing) process. However, knowing that the POP-AuIsocianide precursors possessed medium-to-high specific surface area values and that their catalytic properties were excellent, we could assume that no substantial changes in the porous properties of the materials should be observed when switching from POP-AuIsocianide to its corresponding POP-AuCarbene.

Determination of the Au content was carried out by ICP-OES analysis. The Au content was 30.9% in the model (**M1-AuCarbene**), 17.7% in the polymer (**POP1-AuCarbene**), and 8.6% in the copolymer (**POP2-AuCarbene**). It should be noted that the Au content was also determined approximately by TGA (in an O_2 atmosphere), observing roughly similar values for both methods (Table S1).

Details of the structural, thermal, porous, and morphological properties of the materials are included in section S2.

3.3. Catalytic Testing of the Model and POPs-Au^{I}Carbenes. The selected reaction catalyzed by these AuCarbene materials was the enyne cyclization of dimethyl 2-(3-methyl-2-butenyl)-2-propinylmalonate. For this reaction, the formation of three products is well established: the product **A** of exo cyclization,[67] the diene **B**, arising from isomerization of the endocyclic double bond of **A**,[46] and the product **C**,

https://doi.org/10.1021/acsapm.3c02174
ACS Appl. Polym. Mater. 2024, 6, 2453−2463

Table 1. Porosity Parameters of Precursors POPs and POPs-AuIsocyanide

POP	BET ($m^2\ g^{-1}$)	V_{total}[a] ($cm^3\ g^{-1}$)	$V_{microporous}$[b] ($cm^3\ g^{-1}$)	microporosity[c] (%)	adsorption average pore diameter (nm)
POP1	926	0.53[d]	0.35[e]	66	2.3
POP2	263	0.21[f]	0.20[g]	95	3.2
POP1-AuIsocyanide	323	0.16[h]	0.08[i]	50	2.0
POP2-AuIsocyanide	246	0.15[j]	0.14[k]	93	2.5

[a]Total volume of the pores. [b]Microporous volume of the pores. [c]The microporosity is defined as the $V_{microporous}/V_{total}$ ratio. [d]Pores of less than 102 nm at P/P_0 of 0.98. [e]Pores of less than 0.85 nm at P/P_0 of 0.005. [f]Pores of less than 94 nm at P/P_0 of 0.98. [g]Pores of less than 95 nm P/P_0 of 0.2. [h]Pores of less than 102 nm at P/P_0 0.98. [i]Pores of less than 1.5 nm at P/P_0 of 0.1. [j]Pores of less than 95 nm P/P_0 of 0.98. [k]Pores of less than 1.56 nm at P/P_0 of 0.1.

Table 2. Cyclization Reactions Catalyzed by M1-, POP1-, and POP2-AuCarbenes

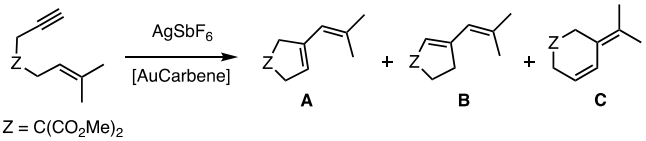

entry	AuCarbene	time (min)	conversion[a] (%)	products (mole ratio)
1[b]	**M1**	1	100	**A**/**B**(60:40)
2[c]	**POP1**	30	51	**A**/**B**/**C**(76:6:18)
3[c]	**POP2**	30	96	**A**/**B**/**C** (81:2:13)
4[c,d]	**POP1**	2	75	**A**/**B**/**C** (77:7:16)
5[c,d]	**POP1**	5	96	**A**/**B**/**C** (74:9:17)
6[c,d]	**POP2**	1	100	**A**/**B**/**C** (85:2:13)

[a]Reaction conditions: in CD_2Cl_2 at 25 °C. The conversion values and percentages of **A**, **B**, and **C** were obtained by ^1H NMR spectrocopy. [b]2 mol % catalyst. [c]4 mol % catalyst. [d]Stirred by using vortex agitation (1 min).

coming from endo cyclization (scheme presented in Table 2).[55,68]

Catalysis tests were performed for the POPs and also for the homogeneous model by employing the methodology cited elsewhere (detailed in section S3).[34−38,42] In the first stage, the catalytic tests were carried out using the following procedure: in an NMR tube was added the corresponding AuCarbene 7

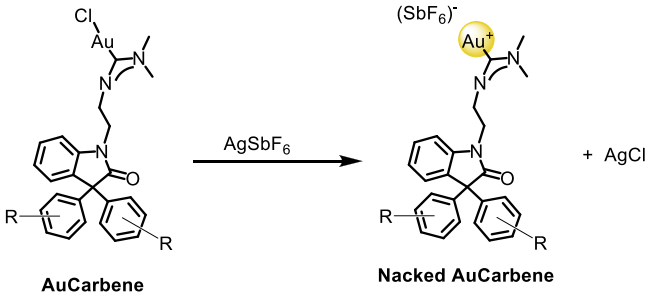

Figure 6. Treatment with $AgSbF_6$ for extraction of the halide in the AuCarbene derivatives.

(2% **M1-AuCarbene**, 4% **POP1-AuCarbene**, or 4% **POP2-AuCarbene**) and an equimolar amount of $AgSbF_6$ to extract the chloride. Figure 6 represents the schematic representation before and after halide extraction in the AuCarbene materials.

Immediately, a solution of dimethyl 2-(3-methyl-2-butenyl)-2-propinylmalonate enyne in 0.5 mL of CD_2Cl_2 was added. The reaction was followed by ^1H NMR with simple stirring of the sample tube (20 rpm) in an NMR device. The catalysis results are shown in Table 1 (entries 1−3). The AuCarbene model **M1-AuCarbene** catalyzed efficiently (100% yield) the skeletal rearrangement of the enyne reagent (entry 1), forming the products **A** and **B** in a 60:40 ratio, while product **C** was not detected. Catalysis was quantitatively achieved in less than 1 min. Even so, it was interesting to observe that the **A**/**B** isomer product ratio changed, in less than 10 min, to a final ratio of 40:60 (Figure S38). Diene **B** is a minor product in the enyne cyclization reaction catalyzed by Au^I complexes, being mainly observed when $FeCl_3$ was employed instead.[36] Thus, the isomerization product **B** was obtained in higher conversion with **M1-AuCarbene** compared to other homogeneous Au^I carbene catalysts reported before.[46] As expected, the kinetics of the heterogeneous Au^I catalysts, **POP1-AuCarbene** (entry 2) and **POP2-AuCarbene** (entry 3), were considerably slower using the same conditions as those of the Au^I model (the enyne took more than 30 min to transform completely). This lower reaction kinetics seems to be possibly due to hindered diffusion of the reagents toward the catalytic centers. In addition, it was observed that the conversions at 30 min of reaction were 51% for **POP1-AuCarbene** (Figure S39) and 96% for **POP2-AuCarbene** (Figure S40), which seems to indicate a higher efficiency of **POP2-AuCarbene** for this cyclization reaction. It should be noted as interesting that, in the case of the confined catalysis, most of the obtained product was **A**, while compound **B** was formed in less than 6% (no observed isomerization even in 30 min), by using both catalytic polymers, showing the heterogeneous catalyst to be more selective than the corresponding homogeneous one. In addition, it was observed that compound **C** was obtained in a higher quantity than that in the case of model catalysis (18 and 13% for **POP1-AuCarbene** and **POP2-AuCarbene** compared to 0% for the model). Thus, these confined catalysts can selectively tune the reaction toward different products, as shown by other heterogeneous catalysts.[4,5]

In order to improve the diffusion of reagents and products, a modified methodology was carried out by stirring the solution before introducing it to the NMR device in a vortex system at 800 rpm for 1 min. The results obtained for the skeletal rearrangement of 1,6-enyne were excellent and are summarized in Table 2 (entries 4−6). In this case, heterogeneous catalysis clearly improved, producing a 100% conversion in less than 5 min for both confined AuCarbene polymer networks: homopolymer (entries 4 and 5, **POP1-AuCarbene**) and copolymer (entry 6, **POP2-AuCarbene**). **POP2-AuCarbene** seemed to be faster, as said before (achieving a quantitative reaction in less than 1 min, whereas **POP1-AuCarbene** showed a 96% conversion in 5 min). Both confined catalysts produced mainly product **A** (74% and 85% for **POP1** and **POP2**, respectively), forming **C** in less than 17% and **B** in less than 9%. Upon comparison with other heterogeneous catalysts described in the literature, the skeletal rearrangement seems to be much faster and more selective under mild condi-

https://doi.org/10.1021/acsapm.3c02174
ACS Appl. Polym. Mater. 2024, 6, 2453−2463

tions.[5,6,44,57] Moreover, it was shown that the heterogeneous catalyst derived from the POPs was much more selective than the homogeneous catalyst model. This fact could be explained by the confinement effect of the catalyst inside the pores of the material. It is worth noting that the FT-IR spectra of POPs-AuCarbenes (after extraction of Cl^-) after a catalytic cycling reaction and washing with dichloromethane produced the same spectrum as the fresh catalyst, confirming survival of the carbene moiety, as denoted by the band at 1566 cm^{-1} (Figure S45).

A second conversion experiment during catalysis was monitored to determine the validity of the catalyst for reuse in more cycles if the activity remained. Table S8 depicts the conversion results. Initially, the reaction after the first addition is too fast (7 min of **POP1-AuCarbene** or 1 min of **POP2-AuCarbene** conducted a total conversion), but that after the second addition is slower, especially for **POP1-AuCarbene**, taking 400 min to consume the enyne (compared to 7 min in the case of **POP2-AuCarbene**). These results are in agreement with the results observed for the first enyne addition. Additionally, a third addition of enyne for **POP2-AuCarbene** was carried out, which was successful and demonstrated that these materials were effective even with successive additions of enyne, which makes it useful for industrial application. Carrying out successive enyne additions, we demonstrated survival of the catalyst, even with the existence of reactants and products in the reaction mixture. This experiment is close to the method employed in flow chemistry, in which the catalyst is embedded and reactants are continuously interacting with the catalyst without the necessity of washing frequently.

The number of catalytic conversions (turnover numbers, TONs) and the frequency of conversions (turnover frequencies, TOFs) for the skeletal rearrangement of dimethyl 2-(3-methyl-2-butenyl)-2-propinylmalonate enyne were determined and are depicted in Table S9. The TON and TOF values employing POPs-AuCarbenes were lower compared to those of an analogous homogeneous catalyst because the diffusion of reactants and products through a microporous material is lower than that in solution.

At this point, it should be noted that the molecular volumes of both the enyne used and the cyclization products (determined by density functional theory calculations) are very similar (enyne has a volume 2−3% higher than that of the cyclization compounds). Therefore, it could be assumed that the inner pores of the material will not suffer from a clogging problem, and therefore no decrease in the effectiveness of the catalytic characteristics will be observed.

3.4. Leaching Testing of POPs-AuCarbenes. To determine the validity of the POPs-AuCarbene as a heterogeneous catalyst, a leaching test was performed to check whether products that could come out of the POP (soluble parts) were those that possess catalytic activity or not. When halide extraction was not performed in the POPs-AuCarbene materials (not treating the POPs-AuCarbene suspension with Ag^I salts), no catalytic activity was observed (Figure S46). Furthermore, to rule out the possibility that other impurities, including those from the solvent, could act as catalysts, the POPs-AuCarbene suspensions were treated with Ag^I salts and filtered. Subsequently, a corresponding amount of enyne was added to the resulting solution. After 40 min of reaction, no cyclization product was observed (Figure S47). In addition, ICP-OES analysis of the filtered solution did not denote the presence of Au. These two experiments confirmed that the catalytic active species of POP are the naked Au^I carbenes, which is formed after removal of the halogen by an Ag^I salt.

3.5. Stability Testing of the Model and POPs-AuCarbenes. The stability test of Au^I carbene was performed following a procedure previously described.[55] Thus, the POPs-AuCarbene and **M1-AuCarbene** were placed in three Schlenk flasks blanketed by N_2, then the Cl^- anion was extracted using

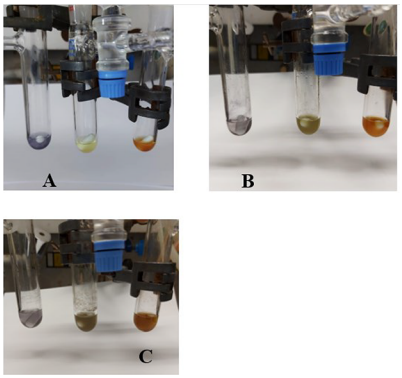

Figure 7. (A) Initially after 3 h of extraction of the halide, (B) after 20 h, and (C) after 15 days: **M1-AuCarbene** (left); **POP1-AuCarbene** (middle); **POP2-AuCarbene** (right).

$AgSbF_6$, and the mixtures were stirred until a purple (darkening for POPs) color appeared, if this was the case, which is indicative of the appearance of Au^0 entities (Figure 7).

As can be seen in Figure 7, the purple color denoting the presence of Au^0 appeared 3 h after extraction of the halide for **M1-AuCarbene**. However, in the case of **POP1-AuCarbene**, it appeared after 20 h, unlike the results seen in the literature, where it was observed that these catalysts,[55] in the absence of a protective ligand, undergo a decomposition process well before 30 min.

This result strongly supports the hypothesis of Au^I disproportionation in Au^0. In microporous polymer networks, where the carbene groups are confined and thus spatially separated, it is more complicated for three Au^I atoms to come together for the disproportionation reaction to occur. However, the presence of Au^0 could be observed, which may indicate either that there is some mobility of Au^I atoms in the structure or that there are certain Au ions not anchored in the carbene units. At this point, we should comment that this was the idea that induced us to prepare the copolymer (**POP2**) with a lower Au^I carbene loading to further separate the Au atoms. The validity of this hypothesis can be observed in the case of **POP2-AuCarbene**, whose decomposition is greatly minimized, making the catalyst stable for more than 15 days.

Surprisingly, in the model, the stability was found to be higher than expected for a homogeneous system without adding any protection agents.[55] A plausible explanation could be that the aliphatic chain has sufficient mobility to place the *naked* Au^I close to the aromatic rings, resulting in additional stabilization. These π Au−arene interactions were previously studied,[69,70] and are known to be strong enough to stabilize the system. Thus, they act as a protecting group, while being weak enough that they can be displaced by the reactant when it binds to the metal, and, consequently, catalysis is observed.

To test the activity of AuCarbenes over time, AuCarbene dispersion (having removed the Cl^-) was maintained for 10

https://doi.org/10.1021/acsapm.3c02174
ACS Appl. Polym. Mater. 2024, 6, 2453−2463

months. Upon dispersion, a series of catalytic tests were performed, observing that both **POP2-AuCarbene** and **POP1-AuCarbene** gave the cyclization products quantitatively (>98%) in less than 5 and 30 min, respectively. However, the **M1-AuCarbene** model did not catalyze efficiently (only 2% of the products were observed). These results seem to confirm the idea that Au^I atoms are confined inside of the microporous polymers, and thus the approach of three Au^I atoms to form Au^0 is severely impeded.

4. CONCLUSIONS

Two microporous organic polymer networks, prepared from TRP and isatin (**POP1**) or an equimolar mixture of 1:1 isatin/TFAP (**POP2**), have been functionalized to give two heterogeneous Au^I catalysts. Functionalization was achieved by introducing a carbene group to the structure, which allowed for confinement of the catalyst inside of the polymer network. Similarly, a homogeneous Au^I carbene catalyst was prepared on an isatin-derived model. Catalytic tests on all heterogeneous and homogeneous systems in the cyclization of a 1,6-enyne have shown that the selectivity of the product formed differs significantly between the homogeneous catalyst and those in which Au^I is confined. It has also been observed that the decomposition to Au^0 that occurs in most catalysis with Au^I-based systems was greatly reduced in the confined materials, probably because there is a greater distance between the Au^I atoms within the polymeric network, which makes it difficult to bring them closer together so that the process of disproportionation can take place. Thus, the **POP2-AuCarbene** copolymer was the polymer that showed the highest long-term stability.

■ ASSOCIATED CONTENT

Supporting Information

The Supporting Information is available free of charge at https://pubs.acs.org/doi/10.1021/acsapm.3c02174.

Experimental section (section S1), characterization of materials (section S2), catalytic experiments (section S3), and bibliography (section S4) (PDF)

■ AUTHOR INFORMATION

Corresponding Author

Jesús A. Miguel − *IU CINQUIMA/Química Inorgánica, Facultad de Ciencias, Universidad de Valladolid, E-47071 Valladolid, Spain;* orcid.org/0000-0003-2814-5941; Email: jamiguel@uva.es

Authors

Sandra Rico-Martínez − *IU CINQUIMA/Química Inorgánica, Facultad de Ciencias, Universidad de Valladolid, E-47071 Valladolid, Spain;* orcid.org/0000-0002-6670-1390

Adrián Ruiz − *IU CINQUIMA/Química Inorgánica, Facultad de Ciencias, Universidad de Valladolid, E-47071 Valladolid, Spain;* orcid.org/0009-0004-6635-4124

Beatriz López-Iglesias − *IU CINQUIMA/Química Inorgánica, Facultad de Ciencias, Universidad de Valladolid, E-47071 Valladolid, Spain*

Cristina Álvarez − *IU CINQUIMA/Química Inorgánica, Facultad de Ciencias, Universidad de Valladolid, E-47071 Valladolid, Spain; Institute for Polymer Science and Technology, Spanish National Research Council (ICTP-CSIC), E-28006 Madrid, Spain; Surfaces and Porous Materials (SMAP, UA-UVA_CSIC), Associated Research Unit to CSIC, University of Valladolid, E-47011 Valladolid, Spain;* orcid.org/0000-0002-5000-0776

Ángel E. Lozano − *IU CINQUIMA/Química Inorgánica, Facultad de Ciencias, Universidad de Valladolid, E-47071 Valladolid, Spain; Institute for Polymer Science and Technology, Spanish National Research Council (ICTP-CSIC), E-28006 Madrid, Spain; Surfaces and Porous Materials (SMAP, UA-UVA_CSIC), Associated Research Unit to CSIC, University of Valladolid, E-47011 Valladolid, Spain;* orcid.org/0000-0003-4209-3842

Complete contact information is available at: https://pubs.acs.org/10.1021/acsapm.3c02174

Author Contributions

The manuscript was written through contributions of all authors. All authors have given approval to the final version of the manuscript. S.R.-M.: methodology, validation, formal analysis, investigation, data curation, writing—original draft, writing—review and editing, and visualization. A.R.: methodology, validation, formal analysis, investigation, data curation, and visualization. B.L.-I.: methodology, validation, investigation, and data curation. C.Á.: resources, writing—review and editing, and funding acquisition. Á.E.L.: resources, methodology, validation, writing—original draft, writing—review and editing, conceptualization, project administration, funding acquisition, and supervision. J.A.M.: resources, methodology, writing—review and editing, conceptualization, project administration, funding acquisition, and supervision.

Funding

This work was supported by Spain's Agencia Estatal de Investigación [Projects PID2019-109403RB-C22 (AEI/FEDER, UE) and PID2020-118547GB-I00 (AEI/FEDER, UE)] and by the Spanish Junta de Castilla y León (VA224P2).

Notes

The authors declare no competing financial interest.

■ ACKNOWLEDGMENTS

The authors thank the ICTP-CSIC services for thermal characterization (TGA) of the polymer materials. Thanks are also due to Dr. Levi López from ICTP-CSIC for the CP/MAS NMR measurements and to Javier Agúndez for the N_2 sorption isotherm experiments. The authors acknowledge LTI (University of Valladolid) for the SEM and TEM images and ICP measurements and CACTI (University of Vigo) for elemental analysis. S.R.-M. thanks Spain's Ministry of Science Innovation and Universities for a FPU grant.

■ ABBREVIATIONS

EAS, electrophilic aromatic substitution; HBHCs, hydrogen-bond-supported heterocyclic carbenes; NACs, N-acyclic carbenes; NHCs, N-heterocyclic carbenes; POP, porous organic polymer; TFAP, trifluoroacetophenone; TFSA, trifluoromethanosulfonic acid; TRP, triptycene

■ REFERENCES

(1) Li, Y.; Yu, J. Emerging Applications of Zeolites in Catalysis, Separation and Host−Guest Assembly. *Nat. Rev. Mater.* **2021**, *6* (12), 1156−1174.

(2) Nakai, Y.; Kimura, T.; Uozumi, Y. Alkylative Cyclization of 1,6-Enynes in Water with an Amphiphilic Resin-Supported Palladium Catalyst. *Synlett* **2006**, *18*, 3065−3068.

(3) Nakai, Y.; Uozumi, Y. Cycloisomerization of 1,6-Enynes: Asymmetric Multistep Preparation of a Hydrindane Framework in Water with Polymeric Catalysts. *Org. Lett.* **2005**, *7* (2), 291−293.
(4) García-Mota, M.; Cabello, N.; Maseras, F.; Echavarren, A. M.; Pérez-Ramírez, J.; Lopez, N. Selective Homogeneous and Heterogeneous Gold Catalysis with Alkynes and Alkenes: Similar Behavior, Different Origin. *ChemPhysChem* **2008**, *9* (11), 1624−1629.
(5) Gryparis, C.; Efe, C.; Raptis, C.; Lykakis, I. N.; Stratakis, M. Cyclization of 1,6-Enynes Catalyzed by Gold Nanoparticles Supported on TiO_2: Significant Changes in Selectivity and Mechanism, as Compared to Homogeneous Au-Catalysis. *Org. Lett.* **2012**, *14* (12), 2956−2959.
(6) Li, Z. X.; Xue, W.; Guan, B. T.; Shi, F. B.; Shi, Z. J.; Jiang, H.; Yan, C. H. A Conceptual Translation of Homogeneous Catalysis into Heterogeneous Catalysis: Homogeneous-like Heterogeneous Gold Nanoparticle Catalyst Induced by Ceria Supporter. *Nanoscale* **2013**, *5* (3), 1213−1220.
(7) Solodenko, W.; Doppiu, A.; Frankfurter, R.; Vogt, C.; Kirschning, A. Silica Immobilized Hoveyda Type Pre-Catalysts: Convenient and Reusable Heterogeneous Catalysts for Batch and Flow Olefin Metathesis. *Aust. J. Chem.* **2013**, *66* (2), 183−191.
(8) Pastva, J.; Skowerski, K.; Czarnocki, S. J.; Žilková, N.; Čejka, J.; Bastl, Z.; Balcar, H. Ru-Based Complexes with Quaternary Ammonium Tags Immobilized on Mesoporous Silica as Olefin Metathesis Catalysts. *ACS Catal.* **2014**, *4* (9), 3227−3236.
(9) Kim, S. W.; Son, S. U.; Lee, S. I.; Hyeon, T.; Chung, Y. K. Cobalt on Mesoporous Silica: The First Heterogeneous Pauson - Khand Catalyst. *J. Am. Chem. Soc.* **2000**, *122* (7), 1550−1551.
(10) Wang, X. D.; Wu, J. J.; Sun, X.; Yang, W. C.; Zhu, J.; Wu, L. Allenylphosphine Oxides as Starting Materials for the Synthesis of Conjugated Enynes: Boosting the Catalytic Performance by MOF Encapsulated Palladium Nanoparticles. *Adv. Synth. Catal.* **2018**, *360* (18), 3518−3525.
(11) Safaei, M.; Foroughi, M. M.; Ebrahimpoor, N.; Jahani, S.; Omidi, A.; Khatami, M. A Review on Metal-Organic Frameworks: Synthesis and Applications. *TrAC - Trends Anal. Chem.* **2019**, *118*, 401−425.
(12) Guo, J.; Jiang, D. Covalent Organic Frameworks for Heterogeneous Catalysis: Principle, Current Status, and Challenges. *ACS Cent. Sci.* **2020**, *6* (6), 869−879.
(13) Geng, K.; He, T.; Liu, R.; Dalapati, S.; Tan, K. T.; Li, Z.; Tao, S.; Gong, Y.; Jiang, Q.; Jiang, D. Covalent Organic Frameworks: Design, Synthesis, and Functions. *Chem. Rev.* **2020**, *120* (16), 8814−8933.
(14) Cai, R.; Ye, X.; Sun, Q.; He, Q.; He, Y.; Ma, S.; Shi, X. Anchoring Triazole-Gold(I) Complex into Porous Organic Polymer to Boost the Stability and Reactivity of Gold(I) Catalyst. *ACS Catal.* **2017**, *7* (2), 1087−1092.
(15) Yang, Y.; Jiang, Y. N.; Lin, Z. Y.; Zeng, J. H.; Liu, Z. K.; Zhan, Z. P. Highly Regio-and Stereo-Selective Heterogeneous 1,3-Diyne Hydrosilylation Controlled by a Nickel-Metalated Porous Organic Polymer. *Org. Chem. Front.* **2021**, *8* (17), 4826−4832.
(16) Zhang, Y.; Riduan, S. N. Functional Porous Organic Polymers for Heterogeneous Catalysis. *Chem. Soc. Rev.* **2012**, *41* (6), 2083−2094.
(17) Nasrallah, H. O.; Min, Y.; Lerayer, E.; Nguyen, T.-A.; Poinsot, D.; Roger, J.; Brandès, S.; Heintz, O.; Roblin, P.; Jolibois, F.; Poteau, R.; Coppel, Y.; Kahn, M. L.; Gerber, I. C.; Axet, M. R.; Serp, P.; Hierso, J. C. Nanocatalysts for High Selectivity Enyne Cyclization: Oxidative Surface Reorganization of Gold Sub-2-Nm Nanoparticle Networks. *JACS Au* **2021**, *1* (2), 187−200.
(18) Dhanalaxmi, K.; Singuru, R.; Mondal, S.; Bai, L.; Reddy, B. M.; Bhaumik, A.; Mondal, J. Magnetic Nanohybrid Decorated Porous Organic Polymer: Synergistic Catalyst for High Performance Levulinic Acid Hydrogenation. *ACS Sustain. Chem. Eng.* **2017**, *5* (1), 1033−1045.
(19) Das, S. K.; Mondal, S.; Chatterjee, S.; Bhaumik, A. N-Rich Porous Organic Polymer as Heterogeneous Organocatalyst for the One-Pot Synthesis of Polyhydroquinoline Derivatives through the Hantzsch Condensation Reaction. *ChemCatChem.* **2018**, *10* (11), 2488−2495.
(20) Chandra, B. K.; Pal, S.; Majee, A.; Bhaumik, A. Ag Nanoparticles Grafted Porous Organic Polymer as an Efficient Heterogeneous Catalyst for Solvent-Free A3 Coupling Reactions. *Mol. Catal.* **2022**, *531*, No. 112686.
(21) Liu, X.; Liu, C. F.; Lai, W. Y.; Huang, W. Porous Organic Polymers as Promising Electrode Materials for Energy Storage Devices. *Adv. Mater. Technol.* **2020**, *5* (9), 1−20.
(22) Rico-Martínez, S.; Álvarez, C.; Hernández, A.; Miguel, J. A.; Lozano, Á. E. Mixed Matrix Membranes Loaded with a Porous Organic Polymer Having Bipyridine Moieties. *Membranes.* **2022**, *12* (6), 547.
(23) Sarkar, C.; Shit, S. C.; Das, N.; Mondal, J. Presenting Porous-Organic-Polymers as next-Generation Invigorating Materials for Nanoreactors. *Chem. Commun.* **2021**, *57* (69), 8550−8567.
(24) Lopez-Iglesias, B.; Suárez-García, F.; Aguilar-Lugo, C.; González Ortega, A.; Bartolomé, C.; Martínez-Ilarduya, J. M.; de la Campa, J. G.; Lozano, Á. E.; Álvarez, C. Microporous Polymer Networks for Carbon Capture Applications. *ACS Appl. Mater. Interfaces* **2018**, *10* (31), 26195−26205.
(25) Esteban, N.; Ferrer, M. L.; Ania, C. O.; de la Campa, J. G.; Lozano, Á. E.; Álvarez, C.; Miguel, J. A. Porous Organic Polymers Containing Active Metal Centers for Suzuki−Miyaura Heterocoupling Reactions. *ACS Appl. Mater. Interfaces* **2020**, *12* (51), 56974−56986.
(26) Vargas, E. L.; Esteban, N.; Cencerrero, J.; Francés, V.; Álvarez, C.; Miguel, J. A.; Gallardo, A.; Lozano, A. E.; Cid, M. B. Pyrrolidine-Based Catalytic Microporous Polymers in Sustainable C=N and C=C Bond Formation via Iminium and Enamine Activation. *Mater. Today Chem.* **2022**, *24*, 100966.
(27) Gandon, V. Modern Gold Catalyzed Synthesis. Edited by A. Stephen K. Hashmi and F. Dean Toste. *Angew. Chemie Int. Ed.* **2012**, *51* (45), 11200−11200.
(28) Hashmi, A. S. K. Gold-Catalyzed Organic Reactions. *Chem. Rev.* **2007**, *107* (7), 3180−3211.
(29) Stratakis, M.; Garcia, H. Catalysis by Supported Gold Nanoparticles: Beyond Aerobic Oxidative Processes. *Chem. Rev.* **2012**, *112* (8), 4469−4506.
(30) Hendrich, C. M.; Sekine, K.; Koshikawa, T.; Tanaka, K.; Hashmi, A. S. K. Homogeneous and Heterogeneous Gold Catalysis for Materials Science. *Chem. Rev.* **2021**, *121* (14), 9113−9163.
(31) Martí, À.; Montesinos-Magraner, M.; Echavarren, A. M.; Franchino, A. H-Bonded Counterion-Directed Catalysis: Enantioselective Gold(I)-Catalyzed Addition to 2-Alkynyl Enones as a Case Study. *Eur. J. Org. Chem.* **2022**, No. e202200518.
(32) Dorel, R.; Echavarren, A. M. Gold(I)-Catalyzed Activation of Alkynes for the Construction of Molecular Complexity. *Chem. Rev.* **2015**, *115* (17), 9028−9072.
(33) Obradors, C.; Echavarren, A. M. Intriguing Mechanistic Labyrinths in Gold(I) Catalysis. *Chem. Commun.* **2014**, *50* (1), 16−28.
(34) Obradors, C.; Echavarren, A. M. Gold-Catalyzed Rearrangements and Beyond. *Acc. Chem. Res.* **2014**, *47* (3), 902−912.
(35) Jiménez-Núñez, E.; Echavarren, A. M. Gold-Catalyzed Cycloisomerizations of Enynes: A Mechanistic Perspective. *Chem. Rev.* **2008**, *108* (8), 3326−3350.
(36) Nieto-Oberhuber, C.; Muñoz, M. P.; López, S.; Jiménez-Núñez, E.; Nevado, C.; Herrero-Gómez, E.; Raducan, M.; Echavarren, A. M. Gold(I)-Catalyzed Cyclizations of 1,6-Enynes: Alkoxycyclizations and Exol Endo Skeletal Rearrangements. *Chem. - A Eur. J.* **2006**, *12* (6), 1677−1693.
(37) Nieto-Oberhuber, C.; López, S.; Jiménez-Núñez, E.; Echavarren, A. M. The Mechanistic Puzzle of Transition-Metal-Catalyzed Skeletal Rearrangements of Enynes. *Chem. - A Eur. J.* **2006**, *12* (23), 5916−5923.
(38) Nieto-Oberhuber, C.; López, S.; Muñoz, M. P.; Cárdenas, D. J.; Buñuel, E.; Nevado, C.; Echavarren, A. M. Divergent Mechanisms for the Skeletal Rearrangement and [2 + 2] Cycloaddition of Enynes

https://doi.org/10.1021/acsapm.3c02174
ACS Appl. Polym. Mater. 2024, 6, 2453−2463

Catalyzed by Gold. *Angew. Chemie - Int. Ed.* **2005**, *44* (38), 6146−6148.
(39) Zhou, Y.-B.; Wang, Y.-Q.; Ning, L.-C.; Ding, Z.-C.; Wang, W.-L.; Ding, C.-K.; Li, R.-H.; Chen, J.-J.; Lu, X.; Ding, Y.-J.; et al. Conjugated Microporous Polymer as Heterogeneous Ligand for Highly Selective Oxidative Heck Reaction. *J. Am. Chem. Soc.* **2017**, *139* (11), 3966−3969.
(40) Cataffo, A.; Peña-López, M.; Pedrazzani, R.; Echavarren, A. M. Chiral Auxiliary Approach for Gold(I)-Catalyzed Cyclizations. *Angew. Chem., Int. Ed.* **2023**, *62*, 1−10.
(41) Alyabyev, S. B.; Beletskaya, I. P. Gold as a Catalyst. Part II. Alkynes in the Reactions of Carbon−Carbon Bond Formation. *Russ. Chem. Rev.* **2018**, *87* (10), 984−1047.
(42) Ferrer, S.; Echavarren, A. M. Role of σ,π-Digold(I) Alkyne Complexes in Reactions of Enynes. *Organometallics* **2018**, *37* (5), 781−786.
(43) Cervantes-Reyes, A.; Rominger, F.; Rudolph, M.; Hashmi, A. S. K. Gold(I) Complexes with Eight-Membered NHC Ligands: Synthesis, Structures and Catalytic Activity. *Adv. Synth. Catal.* **2020**, *362* (12), 2523−2533.
(44) Bartolomé, C.; Ramiro, Z.; Pérez-Galán, P.; Bour, C.; Raducan, M.; Echavarren, A. M.; Espinet, P. Gold(I) Complexes with Hydrogen-Bond Supported Heterocyclic Carbenes as Active Catalysts in Reactions of 1,6-Enynes. *Inorg. Chem.* **2008**, *47* (23), 11391−11397.
(45) Bartolomé, C.; García-Cuadrado, D.; Ramiro, Z.; Espinet, P. Exploring the Scope of Nitrogen Acyclic Carbenes (NACs) in Gold-Catalyzed Reactions. *Organometallics* **2010**, *29* (16), 3589−3592.
(46) Bartolomé, C.; Ramiro, Z.; García-Cuadrado, D.; Pérez-Galán, P.; Raducan, M.; Bour, C.; Echavarren, A. M.; Espinet, P. Nitrogen Acyclic Gold(I) Carbenes: Excellent and Easily Accessible Catalysts in Reactions of 1,6-Enynes. *Organometallics* **2010**, *29* (4), 951−956.
(47) Wang, Y. M.; Kuzniewski, C. N.; Rauniyar, V.; Hoong, C.; Toste, F. D. Chiral (Acyclic Diaminocarbene)Gold(I)-Catalyzed Dynamic Kinetic Asymmetric Transformation of Propargyl Esters. *J. Am. Chem. Soc.* **2011**, *133* (33), 12972−12975.
(48) Handa, S.; Slaughter, L. M. Enantioselective Alkynylbenzaldehyde Cyclizations Catalyzed by Chiral Gold(I) Acyclic Diaminocarbene Complexes Containing Weak Au-Arene Interactions. *Angew. Chemie - Int. Ed.* **2012**, *51* (12), 2912−2915.
(49) Bergamini, G.; Ceroni, P.; Balzani, V.; Gingras, M.; Raimundo, J. M.; Morandi, V.; Merli, P. G. Synthesis of Small Gold Nanoparticles: Au(I) Disproportionation Catalyzed by a Persulfurated Coronene Dendrimer. *Chem. Commun.* **2007**, *1* (40), 4167−4169.
(50) Dinda, J.; Adhikary, S. D.; Seth, S. K.; Mahapatra, A. Carbazole Functionalized Luminescent Silver(I), Gold(I) and Gold(III)−N-Heterocyclic Carbene Complexes: A New Synthetic Disproportionation Approach towards Au(I)−NHC to Provide Au(III)−NHC. *New J. Chem.* **2013**, *37* (2), 431−438.
(51) Dinda, J.; Samanta, T.; Nandy, A.; Saha, K. D.; Seth, S. K.; Chattopadhyay, S. K.; Bielawski, C. W. N-Heterocyclic Carbene Supported Au(I) and Au(III) Complexes: A Comparison of Cytotoxicities. *New J. Chem.* **2014**, *38* (3), 1218−1224.
(52) Dinda, J.; Nandy, A.; Rana, B. K.; Bertolasi, V.; Saha, K. D.; Bielawski, C. W. Cytotoxicity of Silver(I), Gold(I) and Gold(III) Complexes of a Pyridine Wingtip Substituted Annelated N-Heterocyclic Carbene. *RSC Adv.* **2014**, *4* (105), 60776−60784.
(53) Rana, B. K.; Nandy, A.; Bertolasi, V.; Bielawski, C. W.; Das Saha, K.; Dinda, J. Novel Gold(I)- and Gold(III)-N-Heterocyclic Carbene Complexes: Synthesis and Evaluation of Their Anticancer Properties. *Organometallics* **2014**, *33* (10), 2544−2548.
(54) Kumar, M.; Jasinski, J.; Hammond, G. B.; Xu, B. Alkyne/Alkene/Allene-Induced Disproportionation of Cationic Gold(I) Catalyst. *Chem. - A Eur. J.* **2014**, *20* (11), 3113−3119.
(55) Bartolomé, C.; Ramiro, Z.; Peñas-Defrutos, M. N.; Espinet, P. Some Singular Features of Gold Catalysis: Protection of Gold(I) Catalysts by Substoichiometric Agents and Associated Phenomena. *ACS Catal.* **2016**, *6* (10), 6537−6545.
(56) Muratov, K.; Gagosz, F. Confinement-Induced Selectivities in Gold(I) Catalysis—The Benefit of Using Bulky Tri-(Ortho-biaryl)-Phosphine Ligands. *Angew. Chem., Int. Ed.* **2022**, *61* (28), 1−10.
(57) Ben Hadj Hassen, K.; Gaubert, K.; Vaultier, M.; Pucheault, M.; Antoniotti, S. Comparison of Homogeneous and Heterogeneous Ga(III) Catalysis in the Cycloisomerization of 1,6-Enynes. *Green Chem. Lett. Rev.* **2014**, *7* (3), 243−249.
(58) Heitbaum, M.; Glorius, F.; Escher, I. Asymmetric Heterogeneous Catalysis. *Angew. Chemie - Int. Ed.* **2006**, *45* (29), 4732−4762.
(59) Liu, Y.; Lou, B.; Shangguan, L.; Cai, J.; Zhu, H.; Shi, B. Pillar[5]Arene-Based Organometallic Cross-Linked Polymer: Synthesis, Structure Characterization, and Catalytic Activity in the Suzuki−Miyaura Coupling Reaction. *Macromolecules* **2018**, *51* (4), 1351−1356.
(60) Jaśkowska, J.; Kowalski, P. N -Alkylation of Imides Using Phase Transfer Catalysts under Solvent-Free Conditions. *J. Heterocycl. Chem.* **2008**, *45* (5), 1371−1375.
(61) Cheng, L.; Jiang, Z.; Dong, J.; Cai, B.; Yang, Y.; Li, X.; Chen, C. Monolayers of Novel Gemini Amphiphiles with Phthalimide Headgroups at the Air/Water Interface: PH and Alkyl Chain Length Effects. *J. Colloid Interface Sci.* **2013**, *401*, 97−106.
(62) Uson, R.; Laguna, A.; Laguna, M.; Briggs, D. A.; Murray, H. H.; Fackler, J. P. (Tetrahydrothiophene)Gold(I) or Gold(III) Complexes. *Inorg. Synnth.* **1989**, *26* (I), 85−91.
(63) *CrysAlisPro Software System*, version 1.171.33.51; Oxford Diffraction Ltd., Oxford, U.K., 2009.
(64) Sheldrick, G. M. A Short History of SHELX. *Acta Crystallogr. Sect. A Found. Crystallogr.* **2008**, *64* (1), 112−122.
(65) Ortiz-Espinoza, J.; Ruiz-Treviño, F. A.; Hernández-Martínez, H.; Aguilar-Vega, M. J.; Zolotukhin, M. G. Gas Transport Properties in Cross-Linked and Vacuum Annealed Poly(Oxyindole Biphenylylene) Membranes. *Ind. Eng. Chem. Res.* **2018**, *57* (37), 12511−12518.
(66) Kidwai, M.; Jain, A.; Nemaysh, V.; Kumar, R.; Luthra, P. M. Efficient Entry to Diversely Functionalized Spirooxindoles from Isatin and Their Biological Activity. *Med. Chem. Res.* **2013**, *22* (6), 2717−2723.
(67) García-Morales, C.; Echavarren, A. From Straightforward Gold(I)-Catalyzed Enyne Cyclizations to More Demanding Intermolecular Reactions of Alkynes with Alkenes. *Synlett* **2018**, *29* (17), 2225−2237.
(68) Ramiro, Z.; Bartolomé, C.; Espinet, P. Protection of the Gold(I) Catalyst by AsPh3 in Reactions of Enynes. *Eur. J. Inorg. Chem.* **2014**, *2014* (32), 5499−5506.
(69) Schmidbaur, H.; Schier, A. Silver-Free Gold(I) Catalysts for Organic Transformations. *Zeitschrift für Naturforsch. B* **2011**, *66* (4), 329−350.
(70) Herrero-Gómez, E.; Nieto-Oberhuber, C.; López, S.; Benet-Buchholz, J.; Echavarren, A. M. Cationic $\eta1/\eta2$-Gold(I) Complexes of Simple Arenes. *Angew. Chemie Int. Ed.* **2006**, *45* (33), 5455−5459.

https://doi.org/10.1021/acsapm.3c02174
ACS Appl. Polym. Mater. 2024, 6, 2453−2463